Egypt. J. Chem. **Vol. 66,** No. 5 pp. 1 - 14 (2023)

Egyptian Journal of Chemistry

http://ejchem.journals.ekb.eg/

Effects of Synthetic Hierarchical NaP-Zeolite Addition on Physico-mechanical Properties of OPC Hydration Development

Hala A. Hossein, Hanan F. Youssef*

Refractories. Ceramics and Building Materials Department, Advanced Materials Technology and Mineral Resources Research Institute, National Research Centre, El-Behouth St. 12622, Cairo, Egypt.

Abstract

NaP-Zeolite (PZ) can be utilized as pozzolanic material for the improvement of the physico-mechanical, chemical performance and morphological features of cementitious materials. Characterization of PZ was performed using X-ray diffraction, X-ray fluorescence and SEM techniques. This work illustrates the effect of the partial replacement (2.5-20% w/w) of OPC by ZP on the physic-mechanical and chemical characteristics. Water of consistency, setting times, compressive strength, bulk density, total porosity and chemically bound water content results detected that, gradual substitution of OPC by various ratios of PZ enhanced the previous properties at all curing times up to 90-days. Pozzolanic activity of OPC-PZ specimens was confirmed via XRD, SEM and TG/DTG testing that clarified the generation of extra amounts of hydration products such as CSHs and CAHs, which bolsters the physico-mechanical and chemical properties. Obtained outcomes revealed that sample B, including OPC-5% PZ, presented the highest compressive strength, bulk density and chemically bound water contents and the lowest total porosity that were assured by SEM/EDAX images, to clarify more dense and most congested microstructure of platy-like particles of CSHs and CAHs; in addition to, the phase of rode-like shaped crystals of PZ that boosted some micro-reinforcing and filling influences.

Key words: OPC, Na-P Zeolite, Mechanical properties, Compressive strength, Kinetics of hydration.

1. Introduction

The well-known largest carbon footprint especially, CO_2 emitters is cement production which is responsible for more than 5% of total CO_2 emissions and the huge amounts of which come from calcinations of carbonate raw materials [1-3].

Moreover, manufacturing of cement has a conclusive role in the global warming[4]. That is the most produced material in the world, where its annual production is more than 1.6 billion tons; whereas, each 1 ton of Portland cement libates 0.9 ton of CO_2, so that this industry turns into very expensive and consuming for natural resources and energy[5-8].

To understand the chemistry of Portland cement hydration, it is sustainable to consider the hydration processes of all clinker minerals. The results have been showed that there are three distinguished stages of hydration process, (i) the formation of a high CaO/SiO_2 low area intermediate, (*ii*) then transfers to a low CaO/SiO_2, high area intermediate and (iii) the transformation of this to stable hydration products.[9]Many recent efforts focused on the utilization of solid wastes in cement production to reduce the quantities of those wastes, conserve the natural resources and improve the economy[10-13].

It is noteworthy that natural and artificial (agricultural or industrial wastes) pozzolans are not only used in blended cement to reduce energy consumption and CO_2 emission without inspiring any declination to properties of cement but also reuse industrial waste and/or by-products to produce construction material products. Pozzolanic cements are a type of composite cements, where Portland clinker is partially subrogated by supplementary cementitious materials (SCMs) possessing a pozzolanic activity[14, 15].Industrial by-products are

*Corresponding author e-mail: *Corresponding author e-mail: hananeltantawy64@gmail.com, hanan_eltantawy@yahoo.com
Receive Date: 25 February 2022, Revise Date: 07 July 2022, Accept Date: 03 August 2022.
DOI: 10.21608/ejchem.2022.123935.5531

the most popular SCMs such as blast furnace slag[16-18], fly ash[19, 20] and silica fume [21-24],brick waste [25], cement kiln dust [26]and zeolites[27]. SCMs materials react with lime liberated during the hydration of PC producing cementitious materials having hydraulic binder .Pozzolan blended cements have an economical and environmental advantages [28, 29], reduce alkali aggregate reactions [30]and have good resistance against aggressive media[31].

One such material used as fractional substitution of cement is natural or synthetic zeolite, producing hydraulic components of calcium silicate hydrates and calcium aluminate hydrates owing to improvement in the mechanical properties and this characteristic is typical of pozzolan.

It is worth mentioning that, researchers utilize zeolite-bearing tuffs as pozzolans for manufacturing blended cements [32-36]. clinoptilolite, mordenite, phillipsite and chabazite are the most common natural zeolite types in the sedimentary zeolite (tuff) deposits widespread and are excellent pozzolanic materials, often better than pozzolan itself [15, 37]. Zeolites are hydrated aluminosilicate minerals of three-dimensional oxygen-linked $[SiO_4]^{4-}$ and $[AlO_4]^{5-}$tetrahedral frameworks. One of the best applications for zeolites is to be incorporated as supplementary cementitious materials (SCMs). The pozzolanic reaction between zeolites and OPC occurs during (i)hydration of OPC with the liberation of solid $Ca(OH)_2$(ii) dissolution of $Ca(OH)_2$ concerned with equilibria(equations 1&2):

$$Ca(OH)_2s \rightarrow Ca(OH)_l^+ + OH_l^-,(\text{ equation 1})$$

$$Ca(OH)_l^+ \leftrightarrow Ca_l^{2+} + OH_l^-,(\text{equation 2})$$

(iii) cation exchange equilibria including Ca^{2+} and $Ca(OH)^+$ in solution and Na^+ in zeolite(equations 3&4):

$$2\,Na_z^+ + Ca(OH)_l^+ \leftrightarrow Ca_z^{2+} + 2Na_l^+ + OH_l^-,(\text{equation 3})$$

$$2\,Na_z^+ + Ca_l^{2+} \leftrightarrow 2Na_l^+ + Ca_z^{2+},(\text{equation 4})$$

Subscripts s, l and z point out solid, liquid solution and zeolite phase respectively;

(iv)separation and/or of zeolite in alkaline solution to amorphous material put up with the production of calcium silicate hydrates and calcium aluminate hydrates leading to the improvement of mechanical properties of hardened specimens[15, 37]. At ancient times, zeolitic tuff was mixed with lime forming hydraulic binder. In today's building industry, zeolitic tuff can be used as SCMs depending on their chemical composition and microstructure. Due to chemical composition, more siliceous zeolites react faster, expend calcium hydroxide and progress better mechanical properties than those of less siliceous[38-40]. The performance of mechanical properties is due to the combination of reactive silica with calcium hydroxide usually liberates during the hydration of Portland Cement forming calcium silicate hydrate (CSH)[41-43].

Many previous researchers illustrated the effect of the replacement of zeolites by OPC on different characteristics of hardened cement pastes. Ahmadi and Shekarchi showed that, the pozzolanic activity of zeolite was higher than fly ash, but lower than silica fume and the compressive strength of the mixes containing zeolites increased up to 20% zeolite in the presence of suitable amount of superplasticizer[44] .On the other hand, Valipour et al. explained that, the compressive strength of concrete decreased quickly by increasing zeolite amounts in 10-30% of the mass of Portland Cement mix, even though increasing super plasticizer dosage[45].The mechanical properties of concrete containing natural zeolite were investigated by Najimi et al. where, they explained that 15% zeolite developed the compressive strength of concrete but the compressive strength decreased with 30% zeolite even with super plasticizer addition [46].Partial replacement of synthetic zeolite obtained at 95–105 ^{0}C during 1–3 h from aluminium fluoride oxide industrial residue by OPC enhanced the compressive strength and density, and reduced the content of portlandite, total porosity and lower probability of corrosion in hardened cement pastes [47].Besides, the pozzolanic activity of hydro sodalite (zeolite) enabled the formation of hydroaluminate phases in hardened cement paste and had a positive effect on the compressive strength, especially at early hydration process [48].Although having constructive effects, the mixed-type nature, different structures, presence of impurities can negatively influence the strength and durability of concrete admixtures containing natural zeolites, and may result in contrary outcomes in the experimental studies [49]. In this respect, synthetic zeolites can help in the improvement of the cement properties due to uniformly-sized particle and pore sizes, purer product with maintained and tailored

structures, especially if prepared from available local inexpensive resource.

Zeolites of Na-P type is the synthetic analogue of Gismondine natural zeolite (GIS), it shows wide range of compositional changes in the system Na_2O-Al_2O_3-SiO_2-H_2O, and crystallizes in different symmetries at temperatures ranging from 60 up to 250 ^oC, and at least a saturated vapour pressure of 2000 bars [50].

Natural GIS framework type includes gismondine, amicite, gobbinsite, and garronite, meanwhile the synthetic forms contain gobbinsite topology with P2& Pt or tetragonal P, and garronite one with P1&Pc or cubic P [51].

Three polymorphs, or species were reported for NaP zeolite with cubic, tetragonal, and orthorhombic structures. Its topology is made up of two interconnected 8-membered ring channels, having 0.26 x 0.46 nm and 0.31x 044 nm in the [010] and [100] directions, respectively. The spherical colonial gathering crystallization habit of PZ is clearly presented by the aggregation of the tiny crystals (of nano-scale size) in a patchy (Knobbed) sphere [52]. This hierarchical pervious structure of self-assembled NaP-colonial spheres implied not only micro, but also meso and macro-scale pores that can improve the diffusion and facilitate the transportation of the guest cations and other molecules through the structure. Additionally, this crystal habit (spherical aggregation of crystals) is supporting a vast surface area of the zeolite with huge pore vicinities and suppling much more cationic exchange sites on the material surface. PZ was found useful in the treatment of wastewater to eliminate heavy and radioactive elements, some organic particles, and builder in detergents[53].

In the current work, very pure zeolite-P of synthetic origin was prepared from low-cost available Egyptian resource, Kaolin rock, under hydrothermal conditions and used as pozzolanic additives to Portland cement. This presents a good mix design aimed to improve the physico-mechanical and chemical properties of Portland-PZ cement pastes. The hardened pastes containing NaP-zeolite as supplementary cementitious material were investigated.

2. Experimental

2.1. Materials and synthesis of zeolite

The raw materials used in this study include Ordinary Portland cement (OPC) and NaP-zeolite. The Ordinary Portland cement used for sample preparation was afforded from National Cement Company, Helwan, Egypt. Table 1 displays the chemical oxide composition of OPC. The blain surface area of the Portland cement was 3350 cm^2/g.

MEMCO kaolin, CAS-Nr.: 1318-47-7, $Al_2O_7Si_2.2H_2O$, was used as the silica and alumina source for zeolite formation. Table 2 represents the chemical composition of kaolin elemental. Kaolin was calcined at 650 ^oC for 2 hours and reacted with 3.0M NaOH solution with the solid liquid ratio of 1:10. Sodium hydroxide pellets were used as received from Analyzed A.C.S. reagent, a composition of 98.6% NaOH +0.4%Chloride (Baker, SG4031 NT, Sanford, Me, USA). An additional Ludox As-40 colloidal silica of 40% suspension, supplied by Aldrich were used to modify the kaolin composition for meeting the NaP1 zeolite formula, the added rational amount was 1:2.5 for silica: rock. The formed slurry was vigorously stirred for 1h and loaded to a 100 ml Teflon lined vessel (Locally manufactured) and heated at 100 ^oC for 5h in an electric oven. The product was washed severally with distilled water up to pH 7-8 and then dried overnight at 100 ^oC and then be ready for characterization.

Table 1: Chemical oxide composition, (mass. %)

Materials	Oxides									
	SiO_2	Al_2O_3	Fe_2O_3	CaO	MgO	SO_3	Na_2O	K_20	L.O.I	Total
OPC	21.3	5.41	3.77	63.14	1.21	2.35	0.4	0.09	2.57	99.90

Table 2: XRF composition of used Kaolin (wt%)

Oxides contents	Content in Wt %
SiO_2	53.25
Al_2O_3	42.94
TiO_2	1.62
Fe_2O_3	0.41
MgO+CaO+N_2O+SO_3+ Minors	0.03
Total	100

2.2. Characterization techniques of starting raw materials

The chemical compositions of starting materials (OPC and the kaolin) were determined by using X-ray fluorescence method using XRF instrument model AXIOS, WD-XRF sequential spectrometer (Panalytical, 2005). XRD analysis of the prepared NaP-zeolite was analyzed using BRUKUR D_8 ADVANCE with secondary monochromatic beam CuK*a* radiation at 40 Kv and 40 mA. Meanwhile, the internal stricture and crystal morphology of the obtained powder were investigated via scanning electron microscopy (SEM), Philips XL30, attached with EDX unit, with an accelerating voltage 30 kV, magnification up to 400 000 x and resolution for W. 3.5 nm.

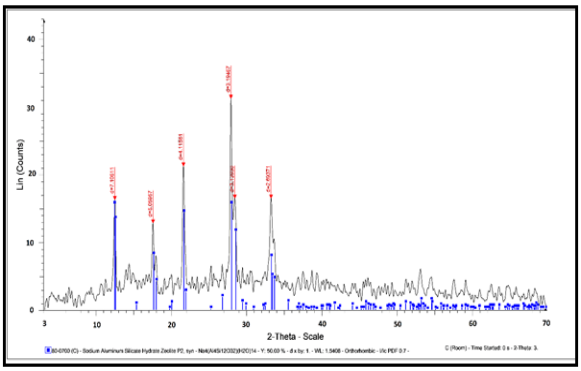

Figure- 1a: XRD for NaP-Zeolite prepared from Egyptian kaolin

Figure 1a, presents the XRD profile of NaP zeolite that was obtained from product heating the slurry at 100 ºC for 5h under hydrothermal conditions). The intensities and positions of peaks were perfectly fitted with the reference card# 80-0700 for sodium aluminium silicate hydrate, zeolite P2, synthetic of the $Na_4(Al_4\ Si_{12}O_{32})14\ (H_2O)$ formula and orthorhombic symmetry. The sharp peaks indicated very well-crystallized layer lattice mineral of the product whereas, the absence of any interfering peaks evidenced a sole and very pure zeolite phase.

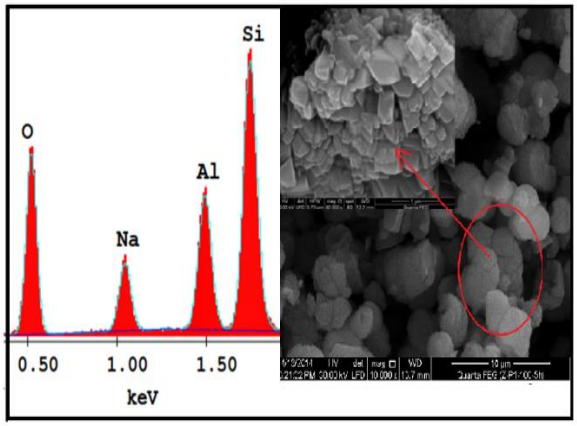

Figure- 1b: SEM for the Knobby, spherical aggregation of nano-zeolite NaP-crystals.

SEM micrographs of the prepared powder showed Knobby spherical aggregation of nano-particles of PZ with rod-like shape, segregated in crystal bundles, as can be seen in Figure 1b. in agreement with the XRD data, the product was a pure Na-P zeolite with no interfering phases. Table 3 presents the chemical composition of the synthetic Na-P species, given by the elemental microanalysis by EDX investigation. It is worth mentioning that, each reading is an average of three analyzed points on the surfaces of three differently-sized Na-P particles. The determined molar Si/Al ratio for the obtained synthetic material was 2.18 which agrees well with literature that limited this percentage to be less than 3 for all P-type zeolites[50, 54, 55]

Table 3: EDX elemental microchemical analysis of Na-P product

Element	Wt%	At%
O K	36.97	49.69
NaK	9.02	8.43
AlK	16.55	13.19
SiK	37.47	28.69
Total	**100**	**100**

2.3. Preparation of NaP-zeolite –OPC pastes

OPC was gradually replaced by PZ, for complete homogeneity, each blend of dry constituent was introduced to a porcelain ball mill for 30 minutes. Five batches composed of those mixtures were designed as illustrated in Table4.

Table 4: Batch compositions of different prepared cements, wt, %

Mix NO.	PC	P zeolite
M_0	100	0
A	97.5	2.5
B	95	5
C	90	10
D	80	20

In this work, the water of consistency (ASTM Designation: C191) [57] and setting time (ASTM C191) [56]were determined. One-inch cubic molds (2.5*2.5*2.5 cm^3) were utilized to attain cubic blended pastes that were kept at 100 % relative humidity (RH) for 24 h. After that, the blended pastes (OPC-NaP-zeolite) were subjected to normal curing (curing under tap water at room temperature).The total porosity and bulk density (ASTM C373-88, C140 and C150)[6, 57, 58]were measured according to the Archimedes rule at each age interval (3, 7, 28 and 90-days of hydration).The mean compressive strength value (for 3 cubes) was also measured(ASTM C109) [59] using automatic hydraulic testing machine type SHIMADZU with maximum capacity 1000 KN and rate of 0.025 KN/ mm^2/s at previous ages of hydration. After that, the crushed specimens of the hardened pastes were ground and the hydration reaction was stopped using stopping mixture (acetone and methanol) with stirring for 1 h. Samples were filtered through a G4, washed two times with diethyl ether and then dried at 80 ^{0}C for 3 h and maintained in a desiccator containing soda lime and CaCl2 until the time of other tests.

The kinetic of hydration were followed by the determination of free lime (ASTM C114) [60] and combined water contents after firing at 950ºC for 30 minutes minus the weight of water in $Ca(OH)_2$.

Some selected samples were examined by the powder method of X-ray diffraction (XRD) using Philis diffractometer PW 1730 with X-ray source of Cu Kα radiation was carried out. The diffractometer was scanned from 5 o to 65 o (2θ) in step size of 0.015 and the counting time per step was 1.8 s. The X-ray tube voltage and current were fixed at 40 KV and 40 mA, respectively. An online search of a standard database (JCPDS database) for X-ray powder diffraction pattern enables phase identification for large variety of crystalline phases in the samples. Thermal analysis of prepared hardened pastes was analysed by Setaram LabsyTMTGDTA16 system between 25 and 1000 ˚C with heating rate of 5˚C/min. Moreover, the microstructural change of those pastes was investigated using Scanning Electron Microscope (JEOL) utilizing secondary electron detectors with energy-dispersive X-ray spectroscopy (EDAX).

3. Results and Discussions:

3.1. Physico-mechanical properties and kinetics of hydration

3.1.1. Water of consistency and setting times

Figure-2 illustrates the initial and final setting times as well as water of consistency (WC) for the blended cement pastes in comparison with the sole OPC pastes. In general, WC was noticeably increased with increasing cement replacement levels. Accordingly, the % replacement of OPC by PZ (finer particles) enhanced the total specific surface area of the blended mixture owing to higher friction and high water demand needed to cover the surface of particles, that is recognized as the "dilution effect of OPC"[1, 39] Furthermore, the substitution of OPC with PZ implied a positive impact on the setting times and by elevating the percentages of PZ, the initial and final setting times were enhanced. It is obvious that, the setting times of OPC pastes were faster than that of OPC-PZ; this trend may be attributed to the dilution effect of OPC with NaP-zeolite. Undoubtedly, as presented in Figure-2, the addition of PZ to OPC caused NaP-zeolite to act as retarding agent for cement pastes.

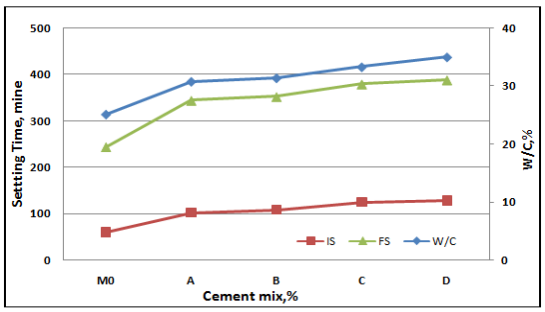

Figure- 2: Water of consistency and setting times of OPC and OPC-P-zeolite pastes.

3.1.2. Compressive strength

Figure-3 presents the compressive strengths of tested formulations as a good mechanical indication for the hydrated OPC and OPC-NaP-zeolite pastes after various hydration times. In general, the compressive strength values for all hardened pastes increased continuously with the hydration times (from 3-days to 90-days);this orientation is due to the hydration evolution of clinker mineral phases[6] and OPC-PZ[43] and formation of calcium silicate hydrates (CSHs) and calcium aluminate hydrates (CAHs). It is clear that, the compressive strength values were elevated by increasing the percentage of PZ (from 2.5 to 10%) at all hydration times (3, 7, 28 and 90-days) and were greater than that of OPC pastes. This enhancement in the strength values may be the result of two reasons; first one which is considered as the main reason is that: as zeolites, like all pozzolanic materials, have contents of SiO_2 and Al_2O_3(from 2.5 to 10% of PZ) that usually accelerate the hydration process and react with $Ca(OH)_2$ liberating during OPC hydration to procedure more dense structure of CSHs and CAHs [61]. The second reason: the presence of rode-like shaped PZ crystals (Figure 1b). The hierarchical assembly of nano-PZ with prismatic or rode-like shaped particles that provided micro-reinforcement over a vast surface area and its combined filler property influenced the texture, leading to dense cement matrix and strengthening the micro structure of the pastes. Besides, a tight interfacial bond might be formed between PZ microfibers and cement owing to higher compressive strength. On the other hand, at higher percentage of PZ (20% replacement), the liberated lime would be decreased, so the amount of additional hydration products formed during the pozzolanic reaction between PZ contents and $Ca(OH)_2$ could not compensate the suppression in the hydration products because of the mitigation influence of OPC. Notably, the addition PZ up to 10% improved the compressive strength values at all curing times due to the previous reasons mentioned before and sample B (5% NaP-zeolite) showed the best and the highest values compared to the other mixes.

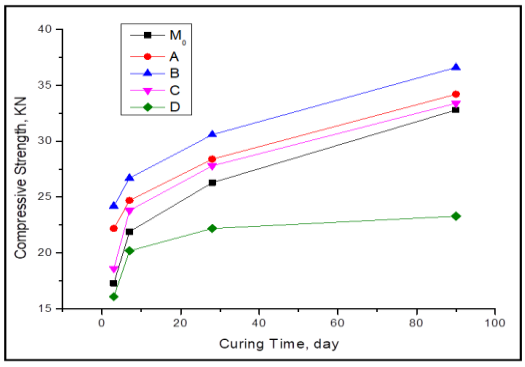

Figure- 3: Compressive strength of hardened ZP cement pastes cured up to 90-days.

3.1.3. Bulk density

Figure-4 clarifies the bulk density values of OPC and OPC-PZ hardened pastes at diverse hydration times (3, 7, 28 and 90-days). Apparently and for all samples; the bulk density values boosted by curing time (from 3 to 90 days) owing to the improvement of the hydration process accompanied by the precipitation of the additional hydration products within the porous matrix. The substitution of OPC with PZ (from 2.5 to 20% replacement) was a reason for marked reduction in the bulk density values at all curing ages of hydration due to the dilution effect of OPC. Moreover, for all blended pastes; the bulk density values increased with increasing PZ percentages up to 5% at all hydration times as a result of the pozzolanic reaction and formation of supplemental hydration yields of CSHs, CAHs, along with the filling and reinforcing effects of PZ gaining more dense structure with greater bulk density, then decreased up to 20% replacement because of extra dilution of OPC. Clearly, sample B (5% NaP-zeolite) presented the highest bulk density values compared to other blended mixes (A, C and D).

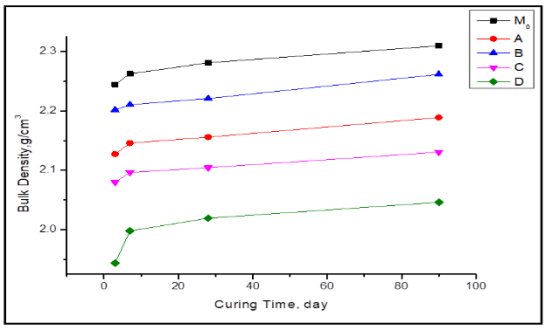

Figure- 4: Bulk density of hardened ZP cement pastes cured up to 90-days

3.1.4. Total porosity

Figure-5 displays the total porosity percentages (%) at various hydration times (3, 7, 28 and 90 days) for OPC and OPC-PZ hardened pastes. Evidently, for all samples the total porosity % reduced by increasing the curing time up to 90-days; this suppression is owing to the formation of supplementary quantities of hydration products inside the pores performing remarkable reduction in the total porosity of hardened pastes [6]. Distinctly, the replacement of OPC by PZ (from 2.5 to 5% in samples A and B) could be attributed to considerable decrease in the total porosity and forming more dense structure at all curing times than that of OPC pastes (M_0); this suppression is due to the same two reasons mentioned formerly. On the other hand, augmentation the % replacement of OPC (from 10 and 20% in samples C and D) led to notable rise in the total porosity % than that of OPC pastes (M_0). Hence, the sample B containing 5% PZ showed the lowest total porosity at all hydration times compared to that of other mixes.

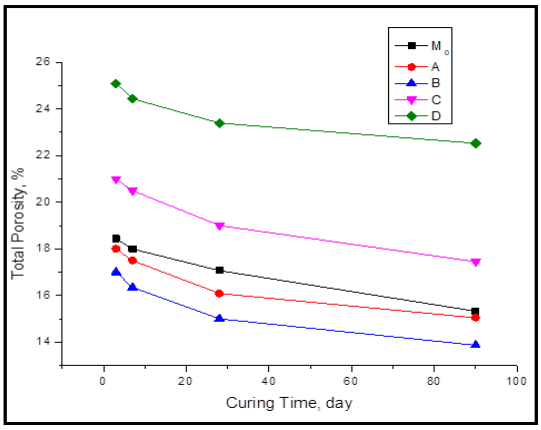

Figure-5: Total porosity of hardened ZP cement pastes cured up to 90-days.

3.1.5. Chemically bound water content

Figure-6 illustrates the chemically bound water contents at various hydration times (3, 7, 28 and 90 days) for OPC and OPC-PZ hardened pastes. In general, the chemically bound water can be applied to know and calculate the hydration degree of cement pastes [2, 62]. Plainly, for all specimens the chemically bound water contents increased with curing ages of hydration up to 90-days; this notable accretion is related to the hydration of clinker mineralogical phases and pozzolanic reaction. Accordingly, the replacement of OPC by PZ (from 2.5 to 10%) commanded to a considerable enhancement in chemically bound water contents at all curing ages than that of M_0 sample (OPC pastes) is attributed to formation of excessive quantities of CSHs and CAHs. In addition, the sample B containing 5% PZ showed the highest chemically bound water contents at all ages of hydration compared to the other mixes. Conversely, sample D (contained 20% NaP-zeolite) presents the lowest chemically bound water contents due to the dilution effect of OPC.

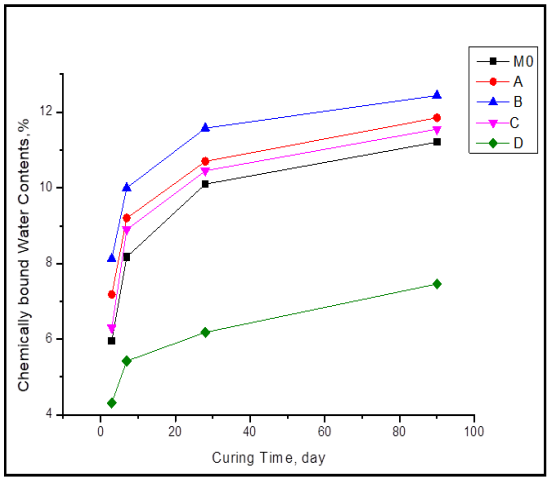

Figure- 6: Chemically bound water contents of hardened ZP Cement pastes cured up to 90-days.

3.2. Phase composition

3.2.1. Mineralogy

Figure-7a clarifies the XRD patterns of OPC-ZP samples A, B, C and D containing 2.5, 5, 10 and 20 P-zeolite% replacements, respectively at 28-days of hydration. The patterns illustrated the characteristic peaks of different hydration products including CSH,$C_3AH_6$and $Ca(OH)_2$ as well as unreacted clinker mineral phases (β-C_2S and C_3S) seen around 32° and 34°in all paste samples [3, 6].
The previous figure presented the existence of PZ rode-like shaped grains that extended micro-reinforcing and filler effects. Obviously; this supplementary phase helped to the development of physic-mechanical properties of these mixes.

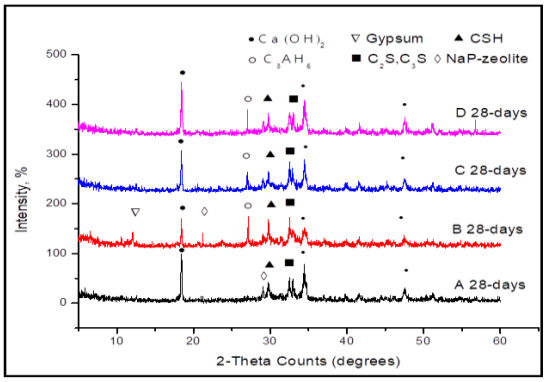

Figure- 7a: X-ray diffraction patterns of hardened OPC-NaP-zeolite pastes at 28-days.

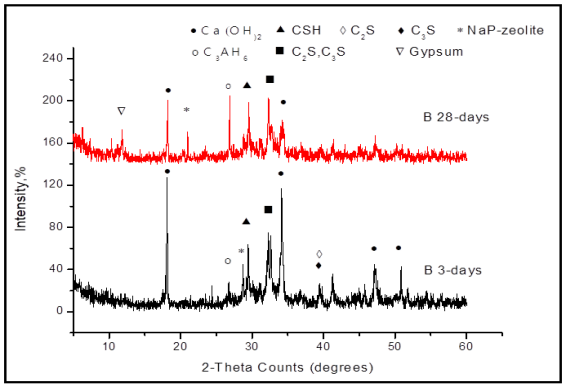

Figure-7b: X-ray diffraction patterns of hardened sample B (contained 5% P-zeolite) at 3 and 28-days.

Figure-7b shows the XRD patterns for sample B contained 5% P-zeolite pastes at 3 and 28-days. It was observed that, the previous peaks for CSH, C_3AH_6, Ca $(OH)_2$, β-C_2S and C_3S were presented in combination with PZ and Gypsum. In addition, the amount of Ca $(OH)_2$, β-C_2S and C_3S decreased from 3 to 28-days; the previous marked suppression is due to the progress of hydration of mineral phases and the pozzolanic reaction of PZ resulted in the creation of excessive amount of hydration products and led to the enhancement of mechanical properties. In this regard, there was notable increase in the peak intensity presenting C_3AH_6 phase in the B-sample at the expenses of the Portlandite Ca $(OH)_2$ones which showed minimal intensity at 28 days. The inverse relation between C_3AH_6 and Ca $(OH)_2$in the cementitious materials can be cleared when considering the known cation exchange property owned for zeolites. Under the hydration condition, the Na^+ cation showed in NaP channels, can readily be replaced by the Ca^{2+} from the portlandite (Ca OH_2), causing its peak deterioration, as seen in Figure 7a-b. In addition, partial instability of the nano-PZ particles against the hydration conditions may subject the more susceptible Al- contents to be detached from the aluminosilicate framework, leading to zeolite skeletal break down. The separated Al can find its way to react and form C_3AH_6, meanwhile, zeolite remaining silica in this case may be precipitated as an amorphous phase that can also interact with the hydration developed materials to form hydrated Ca-silicates. It has been mentioned that, hydrated silicates and aluminates precipitation was one of the functional properties of incorporating zeolites as pozzolanic substances [63].

3.2.2. Microstructure and morphological features

Figure-8 (a1&a2) monitors SEM images that clarifying the microstructure and morphological characteristics of hardened OPC pastes (M_0) after 28-days of hydration. The micrograph of sample M_0 emphasized the existence of small amounts of platy-particles and fibres of CSH intermixed with great quantities of hexagonal crystals of free lime aside from small quantities of unreacted phases and some open pores (Figure-8a1) that were prepared for the precipitation of additional amounts of hydration products. The inhomogeneous nature of such internal construction presented more open structure containing differently-sized particles and interstitial micro, meso, and macro-sized pores spreading all over the scanned areas.

Figure-8(b1& b2) displays the microstructure of sample (OPC-5% PZ) after 28-days of hydration. It is important to emphasize the diverse components produced during hydration process to detect the purpose backwards the improvement of strength. The micrographs illustrated the appearance of extra quantities of hydration products of plates of noteworthy compounds in a cement matrix after hydration in charge of strength are CSHs as a result of pozzolanic reaction. The rode-like PZ particles appeared from those images that extended some micro-reinforcing effects (Figure-8b2). SEM image of B samples containing OPC-5% PZ showed denser microstructure owing to higher ratios of silica and alumina that were documented by EDAX pattern.

Figure-9 (a) shows EDAX analysis of hardened OPC pastes after 28-days of curing. The figure presented diverse percentages of different elements such as carbon, oxygen, calcium, silicon

and aluminium that displayed the eventuality of formation of CSHs and CAHs phases. In comparison, Figure-(9b) clarifies EDAX image of OPC-5% PZ(sample B) after 28-days of hydration, it had the same previous elements but with higher ratios of silica and alumina. This finding agreed well with the SEM data which showed denser microstructure with almost of all pores impacted by the precipitation of the same preceding hydration products that were manifested by the pozzolanic reactions of the used zeolite.

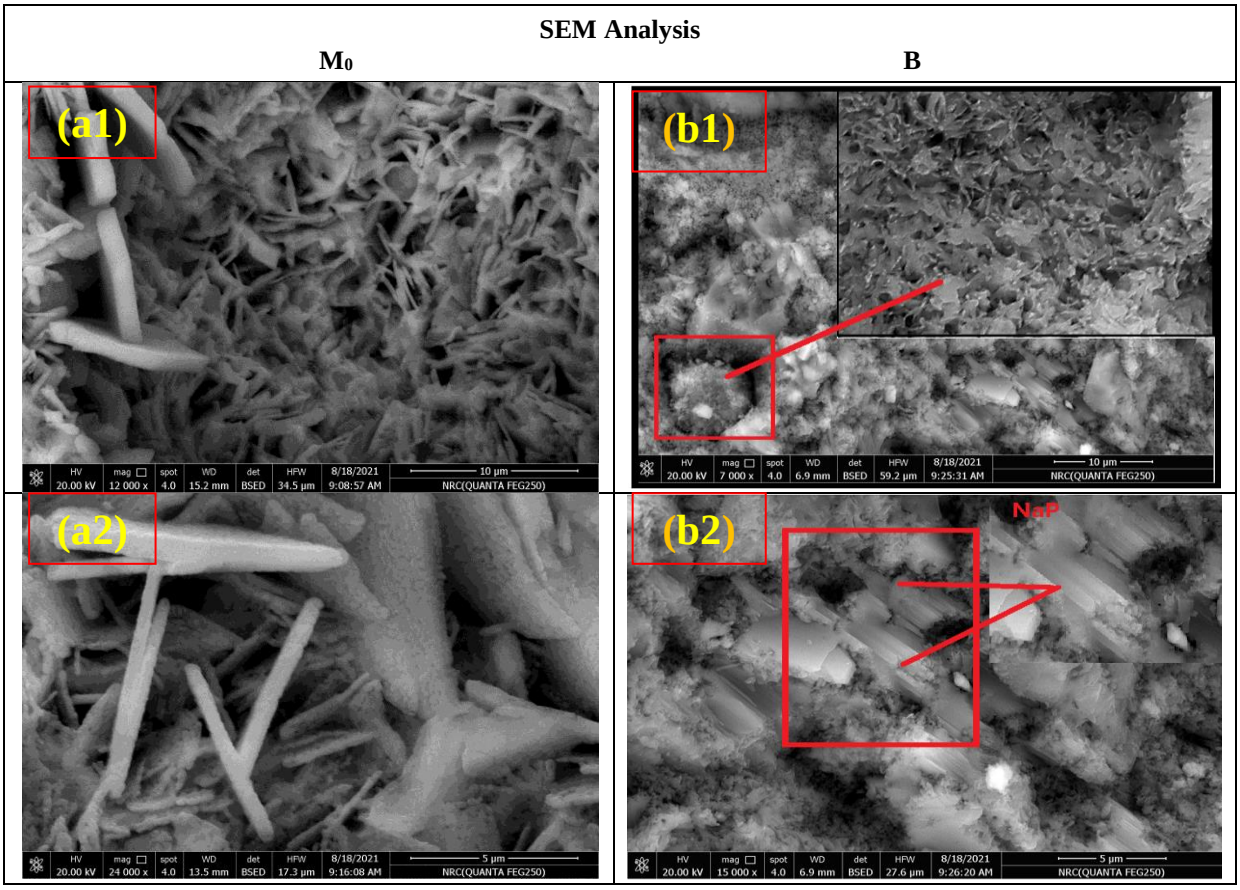

Figure-8: SEM micrographs for hardened samples made from (a1, a2). OPC and (b1, b2) OPC-5% PZ at 28-days of hydration.

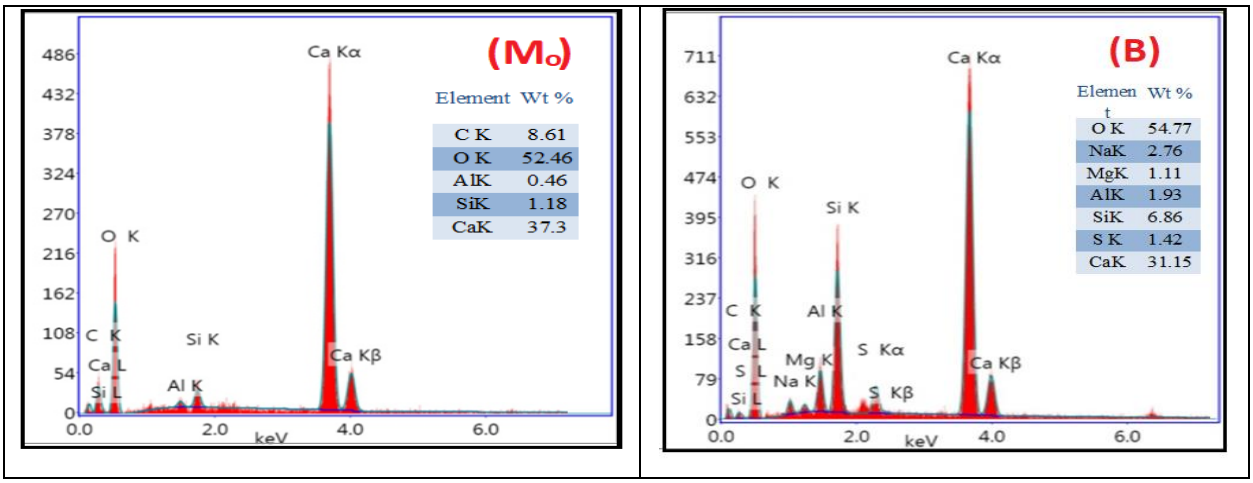

Figure-9: EDX area analyses for hardened samples made from (a) OPC and (b) OPC-5% PZ at 28-days of hydration

3.2.3. Differential thermo gravimetric analysis (TG/DTG)

Figure-10 implies the TG/DTG thermograms for OPC-NaP-zeolite hardened pastes at diverse percentages (5 (B), 10 (C) and 20 (D) %) after 28-days of hydration. It illustrated the existence of endothermic peaks presented at temperature zones of 60-220, 310-420, 420-500, 610-790 and 952 ºC, respectively. The 1st endothermic peak at 50-220 ºC with the maxima at 120 and 176 ºC (in sample B with 5% PZ) was related to the evaporated free and physically adsorbed interlayer water from CSHs gel and secondary hydration products as hydrocalumite (C_4AH_{13}) [6]. Furthermore, the two endothermic peaks were recorded for PZ in the same temperature range of 122 to 191 ºC [64-66] .The 2nd endothermic peaks recorded at 310-420°C with the maximum at 377°C (in sample B) referred to the thermal decomposition of metastable hexagonal phase of calcium aluminate hydrated C_2AH_8),the hydrogarnet phase of C_3ASH_4 and C_3AH_6[67-69].The presence of the first and the second endothermic peaks could be attributed to the pozzolanic reaction and formation of immense amounts of hydration products that improved the mechanical properties of specimen B more than C and D . It was illustrated from Figure-10 that, at 28-days of hydration, the weight loss % up to 200 °C was 6.66 % for B, 18.80 % for C and 17.56 % for D samples; so, B has the lowest weight loss. The elevation in mass depression % may be ascribed to the presence of PZ. Whereas, the % replacement of OPC by PZ (finer particles) increased the total specific surface area of the blended mixture owing to high water demand needed to cover the surface of particles[1, 39].Notably, for zeolites, the loss in weight is usually due to the liberation of the water contained on and within the inner and outer porous surfaces [70, 71].The 3rd pronounced endothermic peak observed at 420-500 ºC with a maximum at 456 ºC supported the dehydroxylation of portlandite phase. The mass depression % of samples B, C and D for this endothermic peak at 28-days of hydration were4.40, 16.21 and 14.55%, respectively. Undoubtedly, the mass depletion percentages were attributed to exhaustion of produced lime via pozzolanic reaction [63];so B has the lowest percentage referred to extra amounts of hydration yields that improved the mechanical properties. Furthermore, this reduction may be related to the dilution influence of OPC with NaP-zeolite so the lime produced during clinker phases hydration will be decreased. The 4thendothermic peaks monitored at 634 and 700 ºC (B), 710 and 760 ºC (C)and 709 ºC (D)clarified the dehydroxylation of MSH gel. The 5th endotherm presented at 952 ºC explained the devastation of calcite phase having diverse proportions of crystallinity. From this figure, it was detected that the total mass reduction proportions of specimens B, C and D were 16.38, 50.77 and 53.47 % at 28-days of hydration respectively**.**

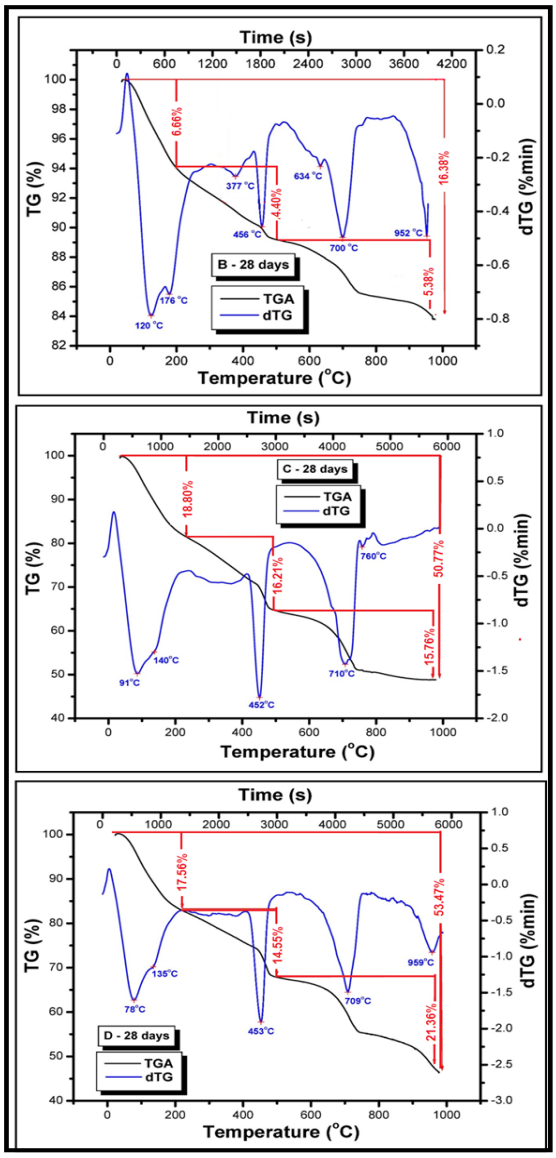

Figure-10: TG/DTG thermograms of hardened pastes of OPC-PZ zeolite with diverse percentages after 28-days of hydration.

4. Conclusions

The influence of substitution of OPC with different ratios of NaP-zeolite on physico-mechanical and chemical characteristics and microstructure were investigated in this article.

The findings from this study can be summarized as follows: -

1- Gradual replacement of OPC with NaP-zeolite up to 20% improved the physico-mechanical properties (compressive strength, total porosity and bulk density) of hardened pastes at all ages of hydration.
2- Addition of NaP-zeolite to OPC heartened the improvement of hardened pastes especially sample B (with 5% PZ) that presented the best physico-mechanical properties as compared to the other samples.
3- XRD and TG/DTG techniques clarified the pozzolanic reaction ascribing to the production of massive amounts of CSHs, CASHs and CAHs at 28-day of hydration.
4- SEM/EDX micrographs confirmed that the implication of 5% PZ (B specimen) in OPC resulted in the production of denser microstructure of platy-like of CSHs and CAHs. In addition, the rode-like shaped crystals of NaP-zeolite particles appeared from those images seemed to extend some micro-reinforcing effects.

Conflicts of interest

There are no conflicts to declare.

Acknowledgement

The authors are giving their direct sincere gratitude to the National Research Institute (Dokki, Cairo, Egypt) for supporting this work.

References

[1] N.A. Nair, V. Sairam, Research initiatives on the influence of wollastonite in cement-based construction material-A review, Journal of Cleaner Production 283 (2021) 124665.

[2] R.I. Khan, W. Ashraf, Effects of ground wollastonite on cement hydration kinetics and strength development, Construction and Building Materials 218 (2019) 150-161.

[3] H. Huang, R. Guo, T. Wang, X. Hu, S. Garcia, M. Fang, Z. Luo, M.M. Maroto-Valer, Carbonation curing for wollastonite-Portland cementitious materials: CO2 sequestration potential and feasibility assessment, Journal of Cleaner Production 211 (2019) 830-841.

[4] B. Yılmaz, A. Uçar, B. Öteyaka, V. Uz, Properties of zeolitic tuff (clinoptilolite) blended Portland cement, Building and environment 42(11) (2007) 3808-3815.

[5] E. Worrell, N. Martin, L. Price, Potentials for energy efficiency improvement in the US cement industry, Energy 25(12) (2000) 1189-1214.

[6] M. Ramadan, S. El-Gamal, F. Selim, Mechanical properties, radiation mitigation and fire resistance of OPC-recycled glass powder composites containing nanoparticles, Construction and Building Materials 251 (2020) 118703.

[7] T.R. Naik, G. Moriconi, Environmental-friendly durable concrete made with recycled materials for sustainable concrete construction, International Symposium on Sustainable Development of Cement, Concrete and Concrete Structures, Toronto, Ontario, October, 2005.

[8] M. Schneider, M. Romer, M. Tschudin, H. Bolio, Sustainable cement production—present and future, Cement and concrete research 41(7) (2011) 642-650.

[9] E.A. Trout, The history of calcareous cements, Lea's Chemistry of Cement and Concrete, 5th Ed., PC Hewlett and M. Liska, Editors (2019) 1-29.

[10] M. Wu, Y. Zhang, G. Liu, Z. Wu, Y. Yang, W. Sun, Experimental study on the performance of lime-based low carbon cementitious materials, Construction and Building Materials 168 (2018) 780-793.

[11] M. Cyr, R. Idir, G. Escadeillas, Use of metakaolin to stabilize sewage sludge ash and municipal solid waste incineration fly ash in cement-based materials, Journal of hazardous materials 243 (2012) 193-203.

[12] W. Ashraf, J. Olek, Carbonation behavior of hydraulic and non-hydraulic calcium silicates: potential of utilizing low-lime calcium silicates in cement-based materials, Journal of materials science 51(13) (2016) 6173-6191.

[13] M.A. Wahab, I.A. Latif, M. Kohail, A. Almasry, The use of Wollastonite to enhance the mechanical properties of mortar mixes, Construction and Building Materials 152 (2017) 304-309.

[14] P. Laniesse, C.C.D. Coumes, A. Poulesquen, A. Bourchy, A. Mesbah, G. Le Saout, P. Gaveau, Setting and hardening process of a wollastonite-based brushite cement, Cement and Concrete Research 106 (2018) 65-76.

[15] D. Caputo, B. Liguori, C. Colella, Some advances in understanding the pozzolanic activity of zeolites: The effect of zeolite structure, Cement and Concrete Composites 30(5) (2008) 455-462.

[16] H. Huang, G. Ye, D. Damidot, Effect of blast furnace slag on self-healing of microcracks in cementitious materials, Cement and concrete research 60 (2014) 68-82.

[17] M.A.E. Aziz, S.A.E. Aleem, M. Heikal, H.E. Didamony, Hydration and durability of sulphate-resisting and slag cement blends in Caron's Lake

water, Cement and Concrete Research 35(8) (2005) 1592-1600.
[18] S. Abd El-Aleem, M. Abd-El-Aziz, M. Heikal, H. El Didamony, Effect of cement kiln dust substitution on chemical and physical properties and compressive strength of Portland and slag cements, The Arabian Journal for Science and Engineering 30(2B) (2005) 263-273.
[19] S. Qian, J. Zhou, E. Schlangen, Influence of curing condition and precracking time on the self-healing behavior of engineered cementitious composites, Cement and concrete composites 32(9) (2010) 686-693.
[20] M. Heikal, H. El-Didamony, T. Sokkary, I. Ahmed, Behavior of composite cement pastes containing microsilica and fly ash at elevated temperature, Construction and building materials 38 (2013) 1180-1190.
[21] P. Youssef, M. El-Feky, M.I. Serag, The Influence of Nano silica surface area on its reactivity in cement composites, Int J Sci Eng Res 8 (2017) 2016-2024.
[22] M. Sahmaran, G. Yildirim, T.K. Erdem, Self-healing capability of cementitious composites incorporating different supplementary cementitious materials, Cement and Concrete Composites 35(1) (2013) 89-101.
[23] J.M. Ortega, M.D. Esteban, R.R. Rodríguez, J.L. Pastor, F.J. Ibanco, I. Sánchez, M.Á. Climent, Influence of silica fume addition in the long-term performance of sustainable cement grouts for micropiles exposed to a sulphate aggressive medium, Materials 10(8) (2017) 890.
[24] E. El-Alfi, A. Radwan, H. Abu-El-Naga, Influence of substitution of ordinary portland cement by silica fume on the hydration of slag-portland cement pastes, Ceramics-Silikaty 55(2) (2011) 147-152.
[25] S.A. Sanad, S.M.A. Moniem, M.L. Abdel-Latif, H.A. Hossein, M.S. El-Mahllawy, Sustainable management of basalt in clay brick industry after its application in heavy metals removal, journal of materials research and technology 10 (2021) 1493-1502.
[26] H.A.-E.-N. Hossein, M.S. Mohammed, E. EL-Alfi, THE ROLE OF CEMENT DUST IN BASALT-DE-ALUMINATED KAOLIN BRICKS, (2006).
[27] M. Cornejo, J. Elsen, C. Paredes, H. Baykara, Hydration and strength evolution of air-cured zeolite-rich tuffs and siltstone blended cement pastes at low water-to-binder ratio, Clay Minerals 50(1) (2015) 133-152.
[28] A. Gineika, R. Siauciunas, K. Baltakys, Synthesis of wollastonite from AlF3-rich silica gel and its hardening in the CO2 atmosphere, Scientific reports 9(1) (2019) 1-10.
[29] N. Demidenko, L. Podzorova, V. Rozanova, V. Skorokhodov, V.Y. Shevchenko, Wollastonite as a new kind of natural material (a review), Glass and ceramics 58(9) (2001) 308-311.
[30] X. Fu, Z. Wang, W. Tao, C. Yang, W. Hou, Y. Dong, X. Wu, Studies on blended cement with a large amount of fly ash, Cement and Concrete Research 32(7) (2002) 1153-1159.
[31] H. Abu-El-Naga, M. Elwan, E. El-Alfi, AGGRESSIVE ATTACK OF SEA WATER ON COMPOSITES CONTAINING METAKAOLIN, (2006).
[32] K. Kitsopoulos, A. Dunham, Heulandite and mordenite-rich tuffs from Greece: a potential source for pozzolanic materials, Mineralium Deposita 31(6) (1996) 576-583.
[33] E.A. Ortega, C. Cheeseman, J. Knight, M. Loizidou, Properties of alkali-activated clinoptilolite, Cement and Concrete Research 30(10) (2000) 1641-1646.
[34] D. Santos, R.L. Santos, J. Pereira, R. Bayão Horta, R. Colaço, P. Paradiso, Influence of Pseudowollastonite on the performance of low calcium amorphous hydraulic binders, Materials 12(20) (2019) 3457.
[35] B. Liguori, D. Caputo, M. Marroccoli, C. Colella, Evaluation of zeolite-bearing tuffs as pozzolanic addition for blended cements, Special Publication 221 (2004) 319-334.
[36] C. Colella, Natural zeolites in environmentally friendly processes and applications, Studies in surface science and catalysis, Elsevier1999, pp. 641-655.
[37] G. Mertens, R. Snellings, K. Van Balen, B. Bicer-Simsir, P. Verlooy, J. Elsen, Pozzolanic reactions of common natural zeolites with lime and parameters affecting their reactivity, Cement and concrete research 39(3) (2009) 233-240.
[38] E. Kontori, T. Perraki, S. Tsivilis, G. Kakali, Zeolite blended cements: evaluation of their hydration rate by means of thermal analysis, Journal of Thermal Analysis and Calorimetry 96(3) (2009) 993-998.
[39] M.H. Cornejo, J. Elsen, H. Baykara, C. Paredes, Hydration process of zeolite-rich tuffs and siltstone-blended cement pastes at low W/B ratio, under wet curing condition, European Journal of Environmental and Civil Engineering 18(6) (2014) 629-651.
[40] S. Antiohos, S. Tsimas, Investigating the role of reactive silica in the hydration mechanisms of high-calcium fly ash/cement systems, Cement and Concrete Composites 27(2) (2005) 171-181.
[41] M. Davraz, L. Gunduz, Engineering properties of amorphous silica as a new natural pozzolan for use in concrete, Cement and Concrete Research 35(7) (2005) 1251-1261.

[42] R. Talero, L. Trusilewicz, A. Delgado, C. Pedrajas, R. Lannegrand, V. Rahhal, R. Mejía, S. Delvasto, F. Ramírez, Comparative and semi-quantitative XRD analysis of Friedel's salt originating from pozzolan and Portland cement, Construction and building materials 25(5) (2011) 2370-2380.
[43] G. Girskas, G. Skripkiūnas, The effect of synthetic zeolite on hardened cement paste microstructure and freeze-thaw durability of concrete, Construction and Building Materials 142 (2017) 117-127.
[44] B. Ahmadi, M. Shekarchi, Use of natural zeolite as a supplementary cementitious material, Cement and concrete composites 32(2) (2010) 134-141.
[45] M. Valipour, F. Pargar, M. Shekarchi, S. Khani, Comparing a natural pozzolan, zeolite, to metakaolin and silica fume in terms of their effect on the durability characteristics of concrete: A laboratory study, Construction and Building Materials 41 (2013) 879-888.
[46] M. Najimi, J. Sobhani, B. Ahmadi, M. Shekarchi, An experimental study on durability properties of concrete containing zeolite as a highly reactive natural pozzolan, Construction and building materials 35 (2012) 1023-1033.
[47] G. Girskas, G. Skripkiūnas, G. Šahmenko, A. Korjakins, Durability of concrete containing synthetic zeolite from aluminum fluoride production waste as a supplementary cementitious material, Construction and building materials 117 (2016) 99-106.
[48] D. Vaičiukynienė, G. Skipkiūnas, V. Sasnauskas, M. Daukšys, Cement compositions with modified hydrosodalite, chemija 23(3) (2012) 147-154.
[49] F.A. Sabet, N.A. Libre, M. Shekarchi, Mechanical and durability properties of self consolidating high performance concrete incorporating natural zeolite, silica fume and fly ash, Construction and Building Materials 44 (2013) 175-184.
[50] A. Taylor, R. Roy, Zeolite studies IV: Na-P zeolites and the ion-exchanged derivatives of tetragonal Na-P, American Mineralogist: Journal of Earth and Planetary Materials 49(5-6) (1964) 656-682.
[51] W.C. BEARD, Linde type B zeolites and related mineral and synthetic phases, ACS Publications1971.
[52] B. Mette, H. Kerskes, H. Drück, H. Müller-Steinhagen, Experimental and numerical investigations on the water vapor adsorption isotherms and kinetics of binderless zeolite 13X, International Journal of Heat and Mass Transfer 71 (2014) 555-561.
[53] Y. Huang, D. Dong, J. Yao, L. He, J. Ho, C. Kong, A.J. Hill, H. Wang, In situ crystallization of macroporous monoliths with hollow NaP zeolite structure, Chemistry of Materials 22(18) (2010) 5271-5278.
[54] D.H. Brouwer, C.C. Brouwer, S. Mesa, C.A. Semelhago, E.E. Steckley, M.P. Sun, J.G. Mikolajewski, C. Baerlocher, Solid-state 29Si NMR spectra of pure silica zeolites for the International Zeolite Association Database of Zeolite Structures, Microporous and Mesoporous Materials 297 (2020) 110000.
[55] J. Kecht, B. Mihailova, K. Karaghiosoff, S. Mintova, T. Bein, Nanosized gismondine grown in colloidal precursor solutions, Langmuir 20(13) (2004) 5271-5276.
[56] S. Amziane, C.F. Ferraris, Cementitious paste setting using rheological and pressure measurements, ACI materials journal 104(2) (2007) 137.
[57] A. ASTM, C373 Standard test method for water absorption, bulk density, apparent porosity, and apparent specific gravity of fired whiteware products, vol. 88, no, Reapproved, 1999.
[58] F.A. Ababneh, A.I. Alakhras, M. Heikal, S.M. Ibrahim, Stabilization of lead bearing sludge by utilization in fly ash-slag based geopolymer, Construction and Building Materials 227 (2019) 116694.
[59] J.K. Norvell, J.G. Stewart, M.C. Juenger, D.W. Fowler, Influence of clays and clay-sized particles on concrete performance, Journal of materials in civil engineering 19(12) (2007) 1053-1059.
[60] P. Sahachaiyunta, K. Pongpaisanseree, J.W. Bullard, P.E. Stutzman, E.J. Garboczi, W. Vichit-Vadakan, Virtual testing in a cement plant, Concrete international 34(9) (2012) 33-39.
[61] D. Novembre, B. Di Sabatino, D. Gimeno, C. Pace, Synthesis and characterization of Na-X, Na-A and Na-P zeolites and hydroxysodalite from metakaolinite, Clay Minerals 46(3) (2011) 339-354.
[62] W. Deboucha, N. Leklou, A. Khelidj, M.N. Oudjit, Hydration development of mineral additives blended cement using thermogravimetric analysis (TGA): Methodology of calculating the degree of hydration, Construction and Building Materials 146 (2017) 687-701.
[63] V. Lilkov, O. Petrov, V. Petkova, N. Petrova, Y. Tzvetanova, Study of the pozzolanic activity and hydration products of cement pastes with addition of natural zeolites, Clay minerals 46(2) (2011) 241-250.
[64] D. Novembre, D. Gimeno, A. Del Vecchio, Synthesis and characterization of Na-P1 (GIS) zeolite using a kaolinitic rock, Scientific reports 11(1) (2021) 1-11.
[65] Z. Huo, X. Xu, Z. Lv, J. Song, M. He, Z. Li, Q. Wang, L. Yan, Y. Li, Thermal study of NaP zeolite with different morphologies, Journal of thermal analysis and calorimetry 111(1) (2013) 365-369.
[66] H.-L. Zubowa, H. Kosslick, D. Müller, M. Richter, L. Wilde, R. Fricke, Crystallization of phase-

pure zeolite NaP from MCM-22-type gel compositions under microwave radiation, Microporous and Mesoporous Materials 109(1-3) (2008) 542-548.
[67] F. Jin, A. Al-Tabbaa, Strength and hydration products of reactive MgO–silica pastes, Cement and Concrete Composites 52 (2014) 27-33.
[68] G.C. Cordeiro, C.P. Sales, Pozzolanic activity of elephant grass ash and its influence on the mechanical properties of concrete, Cement and Concrete Composites 55 (2015) 331-336.
[69] B. Lothenbach, K. Scrivener, R. Hooton, Supplementary cementitious materials, Cement and concrete research 41(12) (2011) 1244-1256.
[70] D. Breck, Zeolite Molecular Sieves Wiley, New York 634 (1974).
[71] O. Korkuna, R. Leboda, b.J. Skubiszewska-Zie, T. Vrublevs'Ka, V. Gun'Ko, J. Ryczkowski, Structural and physicochemical properties of natural zeolites: clinoptilolite and mordenite, Microporous and mesoporous materials 87(3) (2006) 243-254.